

3D HYBRID DEPTH MIGRATION AND FOUR-WAY SPLITTING SCHEMES ^{*1)}

Wen-sheng Zhang Guan-quan Zhang

(LSEC, ICMSEC, Academy of Mathematics and Systems Science, Chinese Academy of Sciences,
Beijing 100080, China)

Abstract

The alternately directional implicit (ADI) scheme is usually used in 3D depth migration. It splits the 3D square-root operator along crossline and inline directions alternately. In this paper, based on the ideal of data line, the four-way splitting schemes and their splitting errors for the finite-difference (FD) method and the hybrid method are investigated. The wavefield extrapolation of four-way splitting scheme is accomplished on a data line and is stable unconditionally. Numerical analysis of splitting errors show that the two-way FD migration have visible numerical anisotropic errors, and that four-way FD migration has much less splitting errors than two-way FD migration has. For the hybrid method, the differences of numerical anisotropic errors between two-way scheme and four-way scheme are small in the case of lower lateral velocity variations. The schemes presented in this paper can be used in 3D post-stack or prestack depth migration. Two numerical calculations of 3D depth migration are completed. One is the four-way FD and hybrid 3D post-stack depth migration for an impulse response, which shows that the anisotropic errors can be eliminated effectively in the cases of constant and variable velocity variations. The other is the 3D shot-profile prestack depth migration for SEG/EAEG benchmark model with two-way hybrid splitting scheme, which presents good imaging results. The Message Passing Interface (MPI) programme based on shot number is adopted.

Mathematics subject classification: 65M06.

Key words: 3D depth migration, Multiway splitting, Data line, Wavefield computation, Finite-difference, Hybrid method.

1. Introduction

Migration is a data processing for oil prospecting in seismic exploration. It gives the images of complex structures by numerical computation of wave propagation. The main step is the downward extrapolation or backward propagation in the subground of wavefield known at surface.

3D prestack depth migration is an important tool for complex structure imaging. There are two kinds of 3D prestack depth migration methods. One is the Kirchhoff integral method which based on ray tracing. The other is the non-Kirchhoff integral method which based on wavefield extrapolation. Kirchhoff integral method is a high-frequency approximation method, which has difficulties in imaging complex structures. However, it can adapt sources and receivers configuration easily and has the advantage of less computational cost. So it is still the dominant method for 3D prestack migration in oil industry. Non-Kirchhoff integral method, such as the finite-difference method, the phase-shift method (Gazdag, 1978), the split-step Fourier (SSF) method (Stoffa et al., 1990) and the Fourier finite-difference (FFD) method (Ristow and Rühl,

* Received November 18, 2004.

¹⁾ This research is supported by the Major State Basic Research Program of Peoples's Republic of China (No.G1999032803), the National Key Nature Science Foundation (No.40004003) and ICMSEC Institute Director Foundation.

1995), all carry out the wavefield extrapolation based on the 3D one-way wave equation. The main step is the downward extrapolation in the subground of a wavefield recorded by receivers at the surface.

For 3D one-way wave equation, a direct solution with stable implicit finite-difference scheme may lead to a non tri-diagonal system, which is computationally expensive. In order to decrease computational cost, the alternatively directional implicit (ADI) scheme is usually used. It splits the finite-difference equation along two directions which are perpendicular to each other, i.e. the 0° and 90° directions, and then implements wavefield extrapolation by solving two tri-diagonal equations successively. By doing so, it saves large computational cost. However, the ADI scheme will lead to azimuthal errors or numerical anisotropic errors with maximum at 45° and 135° . In order to eliminate these errors, Li (1991) derived an error-correction equation to correct the azimuthal anisotropy. Collino and Joly (1995) discussed the operator splitting calculation with the help of power series expansions (Taylor expansion), and they gave a very thorough mathematical derivation of multiway splitting. In 1994, Ristow and Rühl (1994) proposed the ideal of multiway splitting method which splits the migration operator or the square-root operator along three, four and six ways, in order to reduce splitting errors. The commonly used splitting method is a four-way splitting scheme which approximates the square-root operator along 45° and 135° two directions in addition to the original 0° and 90° two directions. However, they all concentrated on the multiway schemes whereas the schemes of wavefield extrapolation in migration are not given. Claerbout (1998) proposed the ideal of helix. Rickett (1998) implemented the implicit 3D wavefield extrapolation with helical boundary conditions. The application of helical conditions simplifies the structure of a finite-difference representation of the Laplacian, reducing the 2D convolution to an equivalent problem in one dimension. The one dimensional filter can be factored into a causal and an anti-causal parts, and the matrix inverse can be computed by recursive polynomial division. Zhang (2000) proposed an explicit four-way scheme in helix but is not unconditionally stable.

In this paper, we will discuss another type of error-correction method, namely the multi-way splitting method on a data line. We implement the computations of wavefield extrapolation on a data line, which makes four-way computations more easily and has a better generality and adaptability. The implicit scheme used in wavefield extrapolation is stable unconditionally. After deriving the relevant formulae and giving the splitting error analysis, numerical analysis for a impulse response with constant and variable velocity are given. And the computations show the correctness of algorithm presented in this paper. Moreover, 3D shot-profile prestack depth migration for SEG/EAEG benchmark model is accomplished and its imaging result show that the traditional ADI hybrid method can yield good images for complexly geological structures.

2. Theory

2.1 FD four-way splitting

The 3D wave equation in the whole space can be written as

$$\frac{1}{v^2} \frac{\partial^2 p}{\partial t^2} - \frac{\partial^2 p}{\partial x^2} - \frac{\partial^2 p}{\partial y^2} - \frac{\partial^2 p}{\partial z^2} = 0, \quad (1)$$

where t denotes time, (x, y, z) are space variables, $p(x, y, z, t)$ is the wavefield, $v(x, y, z)$ is the medium velocity, z is the privileged direction, (x, y) are the transverse variables. Usually, in migration, x denotes the inline direction, y denotes the crossline direction, and z is the depth. In the whole space, the solution of equation (1) can be split into two waves, an upgoing wave and a downgoing wave. They are governed by the 3D one-way wave equation, which has the

following form in the frequency-space domain

$$\frac{\partial \hat{p}}{\partial z} = \pm \frac{i\omega}{v} \sqrt{1 + \frac{v^2}{\omega^2} \left(\frac{\partial^2}{\partial x^2} + \frac{\partial^2}{\partial y^2} \right)} \hat{p} \quad (2)$$

with

$$\hat{p}(x, y, z, \omega) = \int p(x, y, z, t) e^{-i\omega t} dt, \quad (3)$$

where ω is the angular frequency, the plus and minus signs before the square-root operator represent the downgoing wave and upcoming wave respectively. For simplicity here follows, we take the positive sign. We transform equation (2) into the wavenumber k_x, k_y domain where velocity v is assumed to be constant

$$\frac{\partial P}{\partial z} = \frac{i\omega}{v} \sqrt{1 - \frac{v^2}{\omega^2} (k_x^2 + k_y^2)} P \quad (4)$$

with

$$P(k_x, k_y, z, \omega) = \int \int \int p(x, y, z, t) e^{i(k_x x + k_y y - \omega t)} dx dy dt. \quad (5)$$

Formulae (5) can be interpreted as writing the downgoing solution as superposition of harmonic plane waves. A major difficulty with equation (4) is that it corresponds to a non local pseudo-differential equation and therefore is not very tractable from a computational point of view. Several ways can be used to approximate the square-root operator, such as one-order Taylor expansion, rational fraction expansion, Padé approximation and optimal approximation. They all give a local partial differential equation. High-order Taylor expansions are known to give rise to ill-posed problems. The basic form of the approximated square-root operator is

$$\sqrt{1 - s^2} \approx 1 - \frac{\alpha s^2}{1 - \beta s^2}, \quad (6)$$

where $\alpha = 0.5$, $\beta = 0.25$, which yields the so-called 45° paraxial approximation of the square-root operator (Claerbout, 1985).

The square-root operator in equation (4) can be approximated along different directions

$$\begin{aligned} & \sqrt{1 - \frac{v^2}{\omega^2} (k_x^2 + k_y^2)} \\ & \approx \sqrt{1 - \frac{v^2}{\omega^2} k_x^2} + \sqrt{1 - \frac{v^2}{\omega^2} k_y^2} - 1 \\ & \approx \frac{1}{2} \left[\sqrt{1 - \frac{v^2}{\omega^2} k_x^2} + \sqrt{1 - \frac{v^2}{\omega^2} k_y^2} + \sqrt{1 - \frac{v^2}{\omega^2} k_{x'}^2} + \sqrt{1 - \frac{v^2}{\omega^2} k_{y'}^2} \right] - 1, \end{aligned} \quad (7)$$

where k_x and k_y are wavenumber along 0° and 90° directions respectively, whereas $k_{x'}$ and $k_{y'}$ are the wavenumber along 45° and 135° directions. The first approximation expression in (7) is the two-way splitting approximation, and the second is the four-way splitting approximation. Substituting the two-way or four-way approximation into equation (4) and transforming it back to the frequency-space domain, we obtain the following two-way migration equation

$$\frac{\partial P}{\partial z} \approx -\frac{i\omega}{v} P + \frac{i\omega}{v} \left[\sqrt{1 + \frac{v^2}{\omega^2} \frac{\partial^2}{\partial x^2}} + \sqrt{1 + \frac{v^2}{\omega^2} \frac{\partial^2}{\partial y^2}} \right] P \quad (8)$$

and four-way migration equation

$$\begin{aligned} \frac{\partial P}{\partial z} \approx & -\frac{i\omega}{v} P + \frac{i\omega}{2v} \left[\sqrt{1 + \frac{v^2}{\omega^2} \frac{\partial^2}{\partial x^2}} + \sqrt{1 + \frac{v^2}{\omega^2} \frac{\partial^2}{\partial y^2}} \right] P \\ & \frac{i\omega}{2v} \left[\sqrt{1 + \frac{v^2}{\omega^2} \frac{\partial^2}{\partial x'^2}} + \sqrt{1 + \frac{v^2}{\omega^2} \frac{\partial^2}{\partial y'^2}} \right] P, \end{aligned} \quad (9)$$

respectively, where x' and y' are the variables along 45° and 135° directions respectively and can be expressed in terms of x and y by the following expression

$$x' = \frac{\sqrt{2}}{2}(x + y), \quad y' = \frac{\sqrt{2}}{2}(-x + y). \tag{10}$$

Wavefield extrapolation with equation (9) is called four-way splitting scheme. Here, we implement wavefield extrapolation on a data line. Such implementation is suitable to either the conventional finite-difference (FD) or the so-called hybrid method. For the FD method, at each extrapolating depth step, wavefield extrapolation contributes to the following five equations successively in the frequency-space domain

$$\frac{\partial P}{\partial z} = -i\frac{\omega}{v}P, \tag{11}$$

$$\frac{\partial P}{\partial z} = i\frac{\omega}{2v}\sqrt{1 + \frac{v^2}{\omega^2}\frac{\partial^2}{\partial x^2}}P, \quad \frac{\partial P}{\partial z} = i\frac{\omega}{2v}\sqrt{1 + \frac{v^2}{\omega^2}\frac{\partial^2}{\partial y^2}}P, \tag{12}$$

$$\frac{\partial P}{\partial z} = i\frac{\omega}{2v}\sqrt{1 + \frac{v^2}{\omega^2}\frac{\partial^2}{\partial x'^2}}P, \quad \frac{\partial P}{\partial z} = i\frac{\omega}{2v}\sqrt{1 + \frac{v^2}{\omega^2}\frac{\partial^2}{\partial y'^2}}P.$$

With the help of equation (6), the equations (11) and (12) forms the following wavefield extrapolation system

$$\begin{aligned} \frac{\partial P}{\partial z} &= \frac{i\omega}{v}P, \\ \frac{\partial P}{\partial z} &= -\frac{i\omega}{2v}\frac{\alpha v^2}{1-\beta}\frac{\partial^2}{\partial x^2}P, \quad \frac{\partial P}{\partial z} = -\frac{i\omega}{2v}\frac{\alpha v^2}{1-\beta}\frac{\partial^2}{\partial y^2}P, \\ \frac{\partial P}{\partial z} &= -\frac{i\omega}{2v}\frac{\alpha v^2}{1-\beta}\frac{\partial^2}{\partial x'^2}P, \quad \frac{\partial P}{\partial z} = -\frac{i\omega}{2v}\frac{\alpha v^2}{1-\beta}\frac{\partial^2}{\partial y'^2}P. \end{aligned} \tag{13}$$

The numerical examples below show that wavefield extrapolation based on equations (13) can eliminate azimuthal anisotropic errors and thus improve migration precision.

Generally, for wavefield extrapolation of the following equation

$$\frac{\partial P}{\partial z} = LP, \tag{14}$$

where L is a bounded operator in a given Hilbert space with the form of $L = \sum_{i=1}^N L_i$, and n is the splitting number. The exact solution satisfies

$$P(z + \Delta z) = \exp(-iA\Delta z)P(z). \tag{15}$$

Thanks to the expression

$$\exp(-iA\Delta z) = \exp(-iA_1\Delta z)\exp(-iA_2\Delta z)\cdots\exp(-iA_N\Delta z) + O(\Delta z^2), \tag{16}$$

which suggests the approximation

$$P^{n+1} = \exp(-iA_1\Delta z)\exp(-iA_2\Delta z)\cdots\exp(-iA_N\Delta z)P^n, \tag{17}$$

or equivalently

$$\begin{aligned} P_1^n &= \exp(-iA_1\Delta z)P^n, \\ P_2^n &= \exp(-iA_2\Delta z)P_1^n, \\ &\dots\dots \\ P_i^n &= \exp(-iA_i\Delta z)P_{i-1}^n, \\ &\dots\dots \\ P_n^{n+1} &= \exp(-iA_n\Delta z)P_{n-1}^n. \end{aligned} \tag{18}$$

This leads to the following partial differential system

$$\frac{\partial P}{\partial z} = L_i P, \quad i = 1, \dots, n. \quad (19)$$

where $P_i^n (i = 1, 2, \dots, n - 1)$ are the intermediate results.

2.2 Hybrid four-way splitting

Like the derivation of FD four-way splitting scheme, we outline the derivation of hybrid four-way splitting scheme as follows. Introducing a reference velocity $v_0(z)$ and basing on the integral-differential expression of the square-root (Zhang G., 1993)

$$\sqrt{1 - s^2} = 1 - \frac{1}{\pi} \int_{-1}^{+1} \sqrt{1 - \xi^2} \frac{s^2}{1 - \xi^2 s^2} d\xi = 1 - \frac{2}{\pi} \int_0^1 \sqrt{1 - \xi^2} \frac{s^2}{1 - \xi^2 s^2} d\xi. \quad (20)$$

Then, in the frequency domain, one-way downgoing wave equation (4) can be decomposed in the following precise form

$$\frac{\partial P}{\partial z} = (A_1 + A_2 + A_3)P \quad (21)$$

with

$$A_1 = \frac{i\omega}{v_0} \sqrt{1 + \frac{v_0^2}{\omega^2} \left[\frac{\partial^2}{\partial x^2} + \frac{\partial^2}{\partial y^2} \right]}, \quad A_2 = i\omega \left(\frac{1}{v} - \frac{1}{v_0} \right), \quad (22)$$

$$A_3 = \frac{i\omega}{\pi} \int_{-1}^{+1} \left[\frac{v \left(\frac{\partial^2}{\partial x^2} + \frac{\partial^2}{\partial y^2} \right)}{\omega^2 + (sv)^2 \left(\frac{\partial^2}{\partial x^2} + \frac{\partial^2}{\partial y^2} \right)} - \frac{v_0 \left(\frac{\partial^2}{\partial x^2} + \frac{\partial^2}{\partial y^2} \right)}{\omega^2 + (sv_0)^2 \left(\frac{\partial^2}{\partial x^2} + \frac{\partial^2}{\partial y^2} \right)} \right] \sqrt{1 - s^2} ds,$$

where $v_0(z)$ is only a function of z and usually the minimum velocity at each depth step is chosen. The integral expression in equation (22) needs to be approximated by numerical integration. For example, it may be approximated by the Gauss integral formulae (Zhang G., 1993)

$$\frac{1}{\pi} \int_{-1}^0 \sqrt{1 - s^2} f(s) ds \approx \frac{1}{2} \sum_{l=1}^m c_{m,l} f(s_{m,l}). \quad (23)$$

For $m = 1, s_{1,1} = 0, c_{1,1} = 1$, it simplifies 15° one-way wave equation. For $m = 2, s_{2,1} = -s_{2,2} = \frac{1}{2}, c_{2,1} = c_{2,2} = \frac{1}{2}$, it simplifies 45° one-way wave equation.

Therefore, the operator A_3 in equation (22) can be approximated as

$$A_3 \approx i\omega \sum_{l=1}^m c_{m,l} \left[\frac{v \nabla}{\omega^2 + (s_{m,l}v)^2 \nabla} - \frac{v_0 \nabla}{\omega^2 + (s_{m,l}v_0)^2 \nabla} \right] \approx i \frac{\alpha v \nabla}{1 + \beta \frac{v^2}{\omega^2} \nabla}, \quad (24)$$

where, e.g., $\alpha = 0.5(1 - \frac{v_0}{v}), \beta = 0.25(1 + \frac{v_0^2}{v^2})$. ∇ is the Laplacian. In the case of small dip angle, A_3 can be neglected. And for the media with large velocity variations, A_3 should be included. Operators A_1, A_2 and A_3 are termed the phase-shift operator, the time-shift operator and the difference operator (Stoffa et al., 1990; Ristow and Rühl, 1995). Like the wave extrapolation system of FD four-way splitting scheme, the wavefield extrapolation of hybrid four-way splitting scheme can be approximated as

$$\frac{\partial P}{\partial z} \approx (A_1 + A_2 + A_{31} + A_{32} + A_{41} + A_{42})P, \quad (25)$$

where

$$A_1 = \frac{i\omega}{v_0} \sqrt{1 + \frac{v^2}{\omega^2} \left[\frac{\partial^2}{\partial x^2} + \frac{\partial^2}{\partial y^2} \right]}, \quad A_2 = i\omega \left(\frac{1}{v} - \frac{1}{v_0} \right), \quad (26)$$

$$A_{31} = i \frac{\omega}{2v} \frac{\alpha \frac{v^2}{\omega^2} \frac{\partial^2}{\partial x^2}}{1 + \beta \frac{v^2}{\omega^2} \frac{\partial^2}{\partial x^2}}, \quad A_{32} = i \frac{\omega}{2v} \frac{\alpha \frac{v^2}{\omega^2} \frac{\partial^2}{\partial y^2}}{1 + \beta \frac{v^2}{\omega^2} \frac{\partial^2}{\partial y^2}}, \quad (27)$$

$$A_{33} = i \frac{\omega}{2v} \frac{\alpha \frac{v^2}{\omega^2} \frac{\partial^2}{\partial x'^2}}{1 + \beta \frac{v^2}{\omega^2} \frac{\partial^2}{\partial x'^2}}, \quad A_{34} = i \frac{\omega}{2v} \frac{\alpha \frac{v^2}{\omega^2} \frac{\partial^2}{\partial y'^2}}{1 + \beta \frac{v^2}{\omega^2} \frac{\partial^2}{\partial y'^2}}.$$

One notes that the calculation of A_1 may be done after transforming it into the wavenumber domain because of constant velocity $v_0(z)$ at each extrapolation depth step.

2.3 splitting errors

In the following splitting errors of the two-way and four-way splitting schemes are discussed. The error ε for FD four-way application of the FD square-root is

$$\varepsilon = \sqrt{1 - s^2 - t^2} - \frac{1}{2}[\sqrt{1 - s^2} + \sqrt{1 - t^2} + \sqrt{1 - s'^2} + \sqrt{1 - t'^2}] + 1 \tag{28}$$

with

$$s = \frac{v}{\omega}k_x, \quad t = \frac{v}{\omega}k_y, \quad s' = \frac{v}{\omega}k'_x, \quad t' = \frac{v}{\omega}k'_y \tag{29}$$

With equation (6), equation (28) can be approximated as

$$\varepsilon \approx \sqrt{1 - s^2 - t^2} - \frac{1}{2}\left[\frac{\alpha s^2}{1 - \beta s^2} + \frac{\alpha t^2}{1 - \beta t^2} + \frac{\alpha s'^2}{1 - \beta s'^2} + \frac{\alpha t'^2}{1 - \beta t'^2}\right] - 1. \tag{30}$$

If we replace s' and t' by s and t , equations (28) and (30) are those of two-way splitting

$$\varepsilon = \sqrt{1 - s^2 - t^2} - [\sqrt{1 - s^2} + \sqrt{1 - t^2}] + 1, \tag{31}$$

$$\varepsilon = \sqrt{1 - s^2 - t^2} - \left[\frac{\alpha s^2}{1 - \beta s^2} + \frac{\alpha t^2}{1 - \beta t^2}\right] + 1. \tag{32}$$

For the hybrid method, similarly, the four-way splitting error is

$$\begin{aligned} \varepsilon = & p\sqrt{1 - s^2 - t^2} - [\sqrt{1 - p^2s^2 - p^2t^2} + (p - 1) \\ & - \frac{1}{2}\frac{\tilde{\alpha}s^2}{1 - \tilde{\beta}s^2} - \frac{1}{2}\frac{\tilde{\alpha}t^2}{1 - \tilde{\beta}t^2} - \frac{1}{2}\frac{\tilde{\alpha}s'^2}{1 - \tilde{\beta}s'^2} - \frac{1}{2}\frac{\tilde{\alpha}t'^2}{1 - \tilde{\beta}t'^2}]. \end{aligned} \tag{33}$$

where $p = v_0/v$, $\tilde{\alpha} = 0.5(1 - p)$, $\tilde{\beta} = 0.25(1 + p^2)$. And if setting $s = s'$ and $t = t'$, it reduces to the hybrid two-way splitting error

$$\begin{aligned} \varepsilon = & p\sqrt{1 - s^2 - t^2} - [\sqrt{1 - p^2s^2 - p^2t^2} + \\ & (p - 1) - \frac{\tilde{\alpha}s^2}{1 - \tilde{\beta}s^2} - \frac{\tilde{\alpha}t^2}{1 - \tilde{\beta}t^2}] \end{aligned} \tag{34}$$

The accuracy of four-way splitting compared to the two-way splitting is shown in the numerical calculations below. Figure 1 shows the splitting errors induced by the FD two-way splitting scheme in which (a) and (b) are those computed by equations (31) and (32) respectively. Both figure (a) and (b) show the obvious numerical anisotropic errors. Figure 2 shows the splitting errors by the FD four-way splitting scheme in which (a) and (b) are those computed by equations (28) and (30) respectively. One will note that the differences between (a) and (b) both in figure (1) and (2) are very small which shows the good approximation of the square-root of the paraxial 45° approximation, and that in figure 1 the splitting errors of FD two-way splitting scheme are obvious with its maximum in 45° or 135° direction and they behave a rhomb. In figure 2, the FD four-way splitting scheme has removed the splitting errors and the figure shows a good circle symmetry. For the splitting errors of hybrid scheme, they are shown in figure 3, figure 4 and figure 5 for three different p values: $p = 0.2$, $p = 0.5$ and $p = 0.8$, respectively. These three different p values correspond to the three cases of strong, middle and weak lateral velocity respectively. One will note that the hybrid four-way splitting scheme has very good circle symmetry in all three cases and that hybrid two-way splitting scheme also has a bit circle symmetry. One will also note that in hybrid four-way splitting scheme there is an isotropic Laplacian operator, i.e., $\sqrt{1 - \frac{v^2}{\omega^2}(\frac{\partial^2}{\partial x^2} + \frac{\partial^2}{\partial y^2})}$. When there is no lateral velocity variations, the image of hybrid method behaves a perfect circle symmetry.

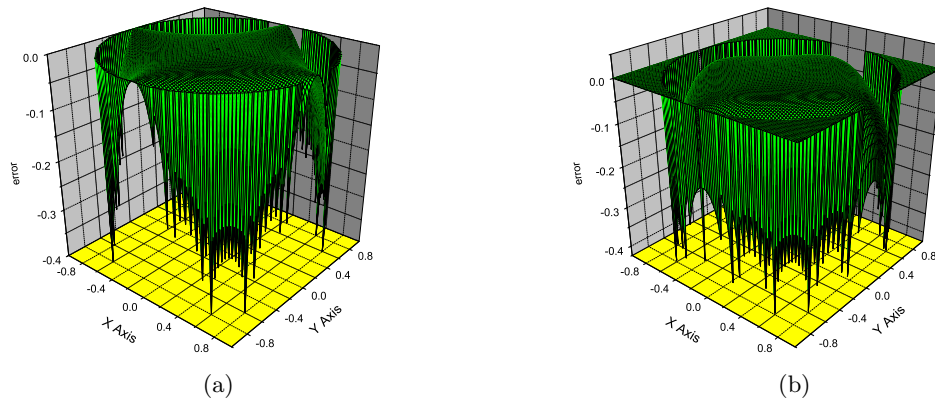


Figure 1. Splitting errors of FD two-way splitting scheme with (a) the precise square-root operator, (b) its 45° paraxial approximation.

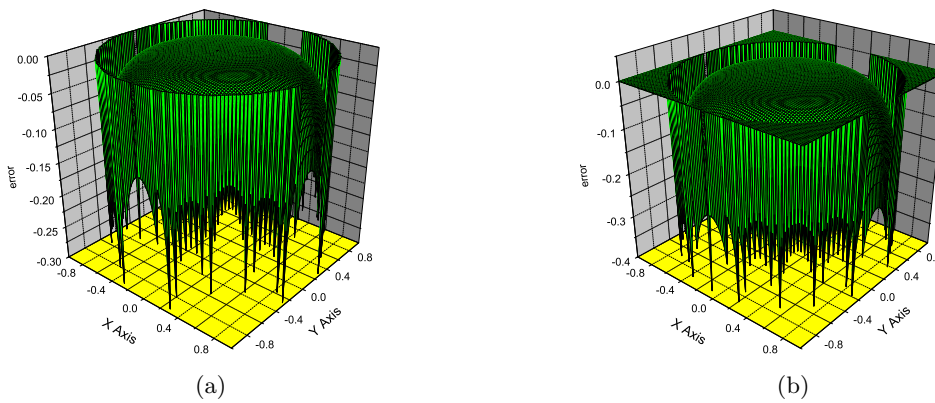


Figure 2. Splitting errors of FD four-way splitting scheme with (a) the precise form of the square-root operator, (b) its 45° paraxial approximation.

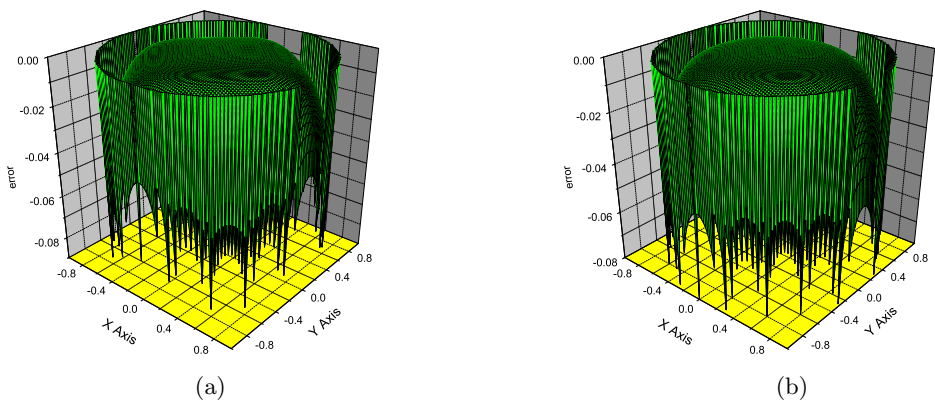


Figure 3. Splitting errors of hybrid method with (a) two-way splitting scheme, (b) four-way splitting scheme for $p = 0.2$.

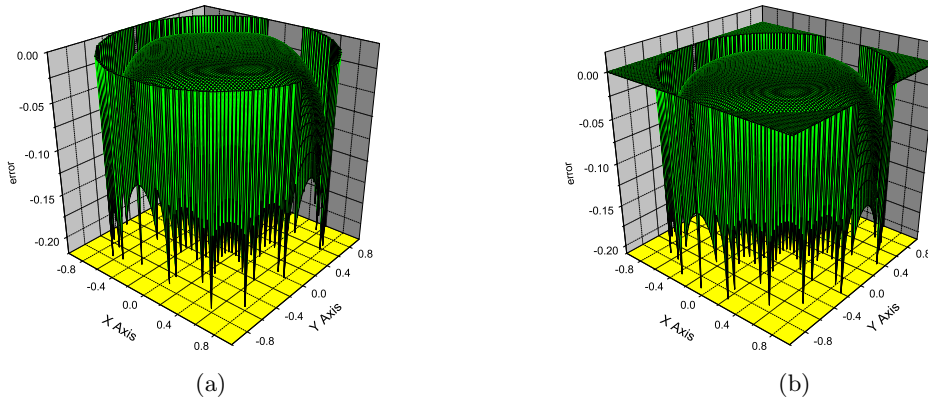


Figure 4. Splitting errors of hybrid method with (a) two-way splitting scheme, (b) four-way splitting scheme for $p = 0.5$.

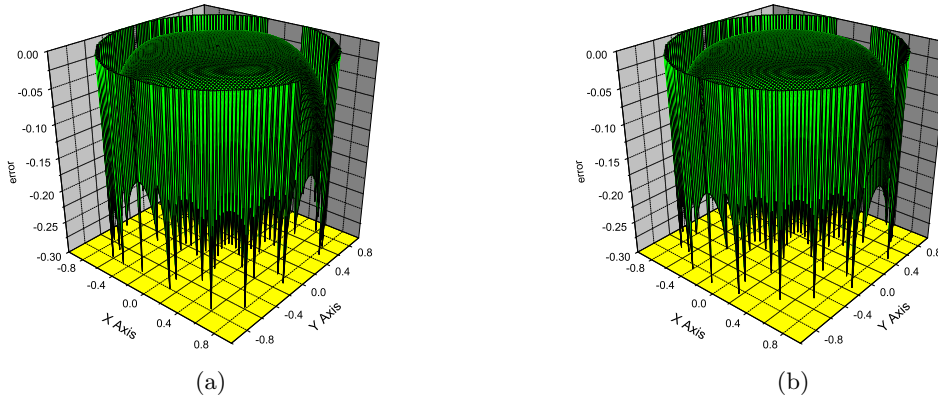


Figure 5. Splitting errors of hybrid method (a) two-way splitting scheme, (b) four-way FFD splitting scheme for $p = 0.8$.

2.4 Four-way wavefield extrapolation on a data line

With the above extrapolation equations of the four-way FD scheme, i.e., equation (13), and the four-way hybrid scheme, i.e., equations (25) to (27), the wavefield extrapolation can be implemented. We implement the four-way wavefield extrapolation on a data line.

We outline the implementation of wavefield extrapolation on a data line with the FD method and the hybrid method as follows. When wavefield extrapolation is implemented along 45° and 135° two directions, one notes that the program complexity arises. However, after introducing an ideal of data line, the difficulty can be overcome. The basic ideal is to transform 2D data into 1D data along a specific direction to form a data line. The wavefield extrapolation based on equation (13) on a data line can be implemented according to the following steps. First of all, the first expression in equation (13) is completed, which is the phase-shift wavefield extrapolation. Then do wavefield extrapolation along 0° and 90° directions with the second and third expressions in equation (13) which contributes to the traditional ADI wavefield extrapolation. And then, arrange the resulting data along 45° direction and do wavefield extrapolation with the fourth expression in equation (13). Finally, arrange the newly resulting data along 135° direction and then do extrapolate wavefield with the last expression in equation (13). By now, the wavefield extrapolation of one depth step is completed and the next depth step can be completed similarly. For wavefield extrapolation of hybrid four-way splitting scheme based

on equations (25) to (27), after finishing the wavefield extrapolation for operators A_1 and A_2 , which are the wavefield extrapolation for the phase-shift operator and time-shift operator respectively, the rest steps of wavefield extrapolation for operators A_{31} , A_{32} , A_{33} and A_{34} are similarly.

In order to improve computational efficiency, one can use the following trick: downward continuation from z to $z + \Delta z$ is performed in two orthogonal directions, then done from $z + \Delta z$ to $z + 2\Delta z$ in two diagonal directions. That is to say, the four-way splitting is replaced by two-fold two-way splitting.

2.5 Wavefield extrapolation with ADI hybrid scheme

For the importance of traditional ADI scheme, we present briefly its difference scheme. The finite-difference equation of ADI hybrid scheme can be derived from the approximated difference operator A_3 of equation (24). The corresponding one-way wave equation for operator A_3 of equation (24) is

$$\frac{\partial P}{\partial z} = i \frac{\alpha \frac{v}{\omega} \left(\frac{\partial^2}{\partial x^2} + \frac{\partial^2}{\partial y^2} \right)}{1 + \beta \frac{v^2}{\omega^2} \left(\frac{\partial^2}{\partial x^2} + \frac{\partial^2}{\partial y^2} \right)}. \quad (35)$$

It is easy to derive that its finite-difference scheme is

$$[1 + (\alpha_1 - i\beta_1)\delta_x^2 + (\alpha_2 - i\beta_2)\delta_y^2]P_{k,l}^{n+1} = [1 + (\alpha_1 + i\beta_1)\delta_x^2 + (\alpha_2 + i\beta_2)\delta_y^2]P_{k,l}^n, \quad (36)$$

where $P_{k,l}^n$ represents $P(k\Delta x, l\Delta y, n\Delta z, \omega)$, δ_x^2 and δ_y^2 are the second-order central difference operators with respect to x and y respectively. And Δx , Δy and Δz are the spatial steps of x , y and z respectively. The coefficients α_1 , α_2 , β_1 and β_2 can be written as

$$\alpha_1 = \frac{\beta v^2}{\omega^2 \Delta x^2}, \quad \alpha_2 = \frac{\beta v^2}{\omega^2 \Delta y^2}, \quad \beta_1 = \frac{\alpha \Delta z v}{2\omega \Delta x^2}, \quad \beta_2 = \frac{\alpha \Delta z v}{2\omega \Delta y^2}. \quad (37)$$

Equation (36) may be solved by the well-known ADI scheme as follows

$$\begin{aligned} [1 + (\alpha_1 - i\beta_1)\delta_x^2]P_{k,l}^{n+1/2} &= [1 + (\alpha_1 + i\beta_1)\delta_x^2]P_{k,l}^n, \\ [1 + (\alpha_2 - i\beta_2)\delta_y^2]P_{k,l}^{n+1} &= [1 + (\alpha_2 + i\beta_2)\delta_y^2]P_{k,l}^{n+1/2}. \end{aligned} \quad (38)$$

Our numerical computations show that this traditional ADI hybrid scheme in 3D shot profile prestack depth migration can yield good images for complex structures.

System (38) is the hybrid two-way splitting scheme. Because the enlarging factor of this difference scheme is always less than one, it is stable unconditionally. For the hybrid four-way difference scheme, with the operator A_{31} , A_{32} , A_{33} and A_{34} in equation (27), we have

$$\begin{aligned} [1 + (\tilde{\alpha}_1 - i\beta_1)\delta_x^2]P_{k,l}^{n+1/4} &= [1 + (\tilde{\alpha}_1 + i\beta_1)\delta_x^2]P_{k,l}^n, \\ [1 + (\tilde{\alpha}_2 - i\beta_2)\delta_y^2]P_{k,l}^{n+2/4} &= [1 + (\tilde{\alpha}_2 + i\beta_2)\delta_y^2]P_{k,l}^{n+1/4}, \\ [1 + (\tilde{\alpha}_1 - i\beta_1)\delta_{x'}^2]P_{k,l}^{n+3/4} &= [1 + (\tilde{\alpha}_1 + i\beta_1)\delta_{x'}^2]P_{k,l}^{n+2/4}, \\ [1 + (\tilde{\alpha}_2 - i\beta_2)\delta_{y'}^2]P_{k,l}^{n+1} &= [1 + (\tilde{\alpha}_2 + i\beta_2)\delta_{y'}^2]P_{k,l}^{n+3/4}, \end{aligned} \quad (39)$$

where $\tilde{\alpha}_1 = \alpha_1/2$ and $\tilde{\alpha}_2 = \alpha_2/2$. The extrapolation with equation (39) is also stable unconditionally. The known boundary conditions is the data $P(x, y, z = 0, t)$ observed or recorded at surface.

The imaging result $M(x, y, z)$ of prestack migration can be obtained by the summing all frequency of the product of the upcoming wave $P(x, y, z, \omega)$ and downgoing $D(x, y, z, \omega)$, i.e.,

$$M(x, y, z) = \sum_{\omega} P(x, y, z, \omega) \bar{D}(x, y, z, \omega) \quad (40)$$

where \bar{D} represents the complex conjugate of D . For the poststack migration, it reduce to sum all the frequency of upcoming wavefield.

3. Numerical Calculations

3.1 Four-way FD and hybrid 3D post-stack depth migration

In order to demonstrate effects of the schemes in this paper, the migration for an impulse response is presented first. The grid number for x , y and z is 64, the spatial step for x and y is 15m. The extrapolation step is 15m. The time sampling step is 4ms. The medium velocity is 3000m/s. It is well known that the theoretical 3D migration result in homogeneous media is a half sphere. The impulse is the Ricker wavelet with 20Hz main frequency which located at the position of $(x, y, z, t) = (480m, 480m, 500ms)$. Figure 6(a) is the horizontal slice of migration result by the traditional FD two-way splitting scheme, which shows that the migration errors caused by different azimuthal angles reach maximum along 45° and 135° directions. Figure 6(b) is the slice by FD two-way splitting scheme but splitting along 45° and 135° two directions, which shows the migration errors reach maximum along 0° and 90° directions. And figure 6(c) is that by four-way splitting scheme along 0°, 90°, 45° and 135° four directions, which shows a perfect circle symmetry like theoretical predication.

For the media with constant velocity, due to equality of the reference velocity with the constant media velocity, there is only the phase-shift operator in the hybrid method in fact. That is to say, there are no any actual extrapolations for the rest time-shift operator A_2 and the difference operators A_{31} , A_{32} , A_{33} and A_{34} . In this case, the migration result is a precise hemisphere because the Laplacian is an isotropic operator. Thus there is no azimuthal errors when the four-way scheme is used for the media with constant velocity. Let's consider the case of variable velocity. Suppose the velocity is $v(x, y, z) = 1600 + 3x + 3y + z(m/s)$. The parameter p in hybrid formula varies from 0.46 to 0.57. The spatial steps and the other parameters are the same with those of the FD example with constant velocity in this subsection. Figure 7 are the horizontal slices of the 3D migration result at $z = 280m$, which calculated by the hybrid method of the two-way splitting scheme and the four-way splitting scheme respectively. Figure 7(a) is the result by the traditional two-way splitting scheme. Figure 7(b) is that by the two-way splitting scheme but splitting along 45° and 135° two directions. Figure 7(c) is that by the four-way splitting scheme. Comparisons between figure 7(a) and figure 7(c) show that the numerical anisotropic errors of traditional two-way scheme is also eliminated.

3.2 ADI 3D prestack depth migration

The SEG/EAGE salt model is an international 3D benchmark model. The data used here has the 50 shot lines with 160m line space. Each line has 96 shots with 80m shot space. Each shot has 68×6 receivers. The grid element is 40m×40m. The record length is 4992ms with 8ms time step. The model amount is about 6.23 Gbytes. In this large scale computation, the MPI programming is adopted to improve computational efficiency. Here, x denotes the inline direction and y the crossline direction. The 3D shot-profile prestack depth migration by ADI hybrid scheme is completed. Figure 8(a) is the vertical slice of 3D velocity model at $x = 5400m$ and figure 8(b) is the vertical slice of the migration result. Figure 8 shows that the ADI hybrid method yields good images of the model at the same position. In all calculations, the MPI parallel algorithm is adopted. And shot number is chosen as parallelization parameter for single-shot profile migration. The parallel efficiency is very high because the problem itself has very high parallel feature.

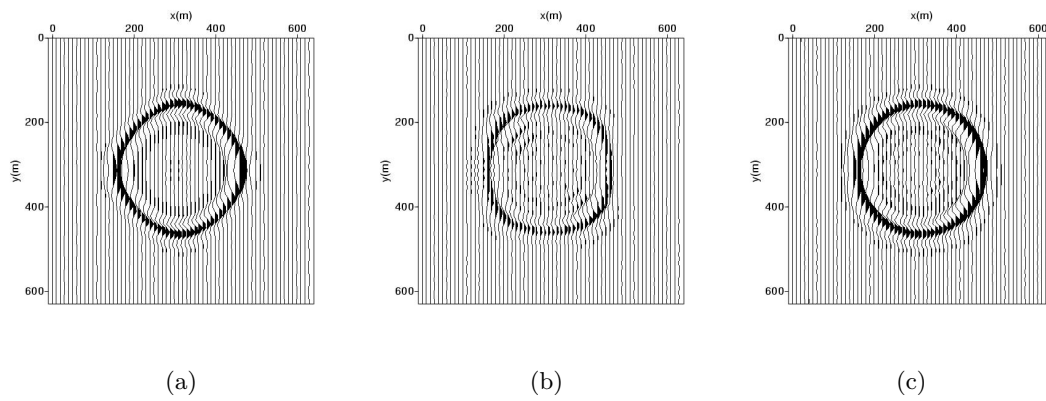


Figure 6. Horizontal slices of 3D post-stack depth migration for a impulse response with constant velocity. FD method with (a) traditional two-way splitting, (b) 45° and 135° two-way splitting, (c) Four-way splitting.

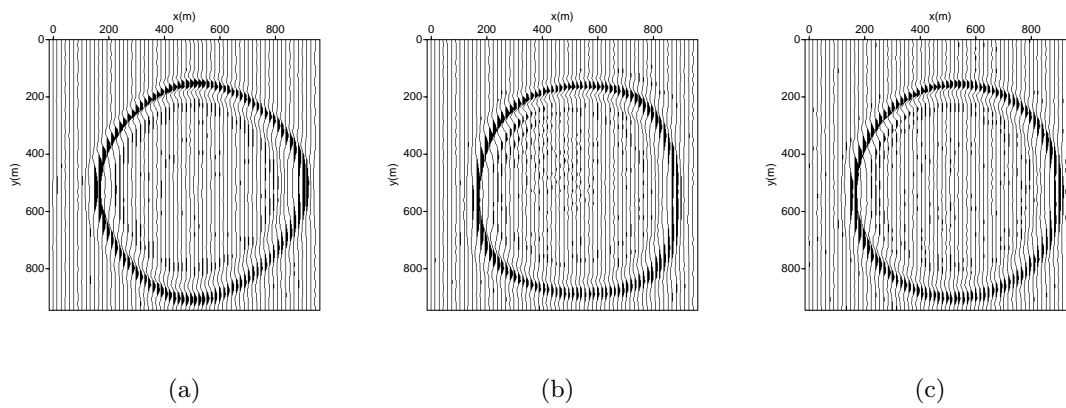


Figure 7. 3D post-stack depth migration for a impulse response with variable velocity. Hybrid method with (a) traditional two-way splitting, (b) 45° and 90° two-way splitting, (c) four-way splitting.

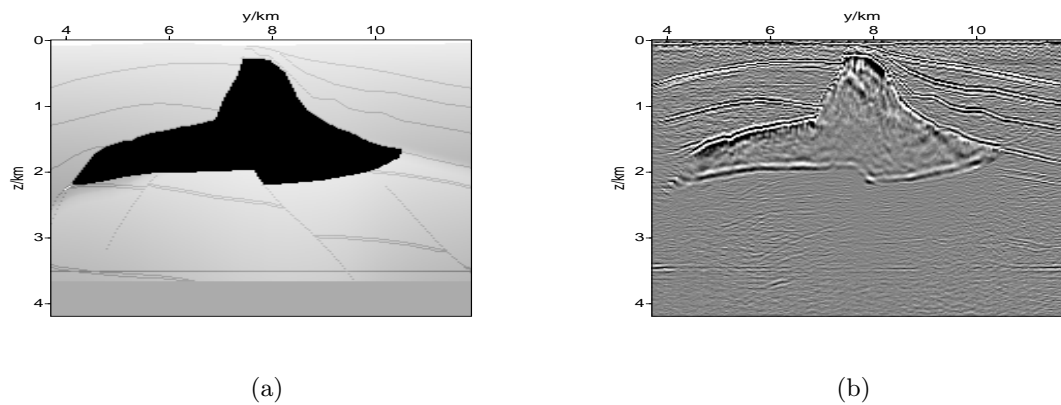


Figure 8. The vertical slices at $x = 5400m$ along crossline direction. (a) a slice of 3D velocity model, (b) a slice of 3D shot-profile prestack migration with two-way hybrid method.

4. Conclusions

Based on the ideal of data line, the four-way splitting schemes and extrapolation equations for FD and hybrid methods are derived. The advantage of wavefield extrapolation on a data line is unconditionally stable. Numerical calculations show that the four-way FD algorithms can eliminate numerical anisotropic errors effectively. Moreover, the numerical anisotropic errors of hybrid method is less than that of FD. The traditional ADI hybrid method is preferred in 3D shot-profile prestack depth migration in order to save computational time for the media with low lateral velocity variations. And our experience show that the traditional ADI hybrid method also can yield good images even in middle lateral velocity variations. The 3D shot-profile prestack depth migration for SEG/EAGE salt model with ADI hybrid method is implemented and good imaging results are obtained. The Message Passing Interface (MPI) programme based on shot number is adopted. Each processor has the same shot number to carry out 3D prestack depth migration. Therefore the parallel speedup ratio is high and the computational efficiency is improved further. The scheme in this paper has potential practical values.

References

- [1] Claerbout, J.F. Multidimensional recursive filters via a helix, *Geophysics*, **63**:5 (1998), 1532–1541.
- [2] Claerbout, J.F. Imaging the earth's interior, Blackwell, Oxford, 1983.
- [3] Collina, F. and Joly, P. Splitting of operators, alternated directions, and paraxial approximations for the three-dimensional wave equation, *SIAM J. Sci. Comput.*, **16** (1995), 1019–1048.
- [4] Li Z., Compensating finite-difference errors in 3-D migration and modeling, *Geophysics*, **56**:10 (1991), 1650–1660.
- [5] Gazdag, J. Wave equation migration with the phase-shift method, *Geophysics*, **43**:7 (1978), 1342–1351.
- [6] Gazdag, J. and Sguazzero, P. Migration of seismic data by phase shift plus interpolation, *Geophysics*, **49**:3 (1984), 124–131.
- [7] Rickett, J., Claerbout, J. and Fomel, S., Implicit 3-D depth migration by wavefield extrapolation with helical boundary conditions 68th SEG Meeting, 1999, Expanded Abstracts, 1124–1127.
- [8] Ristow, D. and Rühl, T. Fourier finite-difference migration, *Geophysics*, **59**:12 (1995), 1882–1893.
- [9] Ristow, D. and Rühl, T. 3-D implicit finite-difference migration by multiway splitting, *Geophysics*, **62**:2 (1997), 554–567.
- [10] Stoffa, P. L., Forkema, J. T., de Luna Freire, R. M., et al. Split-step Fourier migration, *Geophysics*, **55**:4 (1990), 410–421.
- [11] Zhang Guanquan. Coupled equations of wave equation for upgoing wave and downgoing wave, *Acta Applied Maths*, **16** (1993), 251–263.
- [12] Zhang Guanquan, San Guojian and Zhang Wensheng. 3-D Post-stack depth migration in helical coordinate system. SEG/SPE International Symposium on Reservoir Geophysics, Shengzhen, People's Republic of China, Dec.4-10, 2000, Expanded abstracts, 158–166.